research articles Journal of proteome research

Proteomic Identification of Differentially Expressed Proteins in the *Ligon lintless* Mutant of Upland Cotton (*Gossypium hirsutum* L.)

Pi-Ming Zhao,[†,‡,§] Li-Li Wang,[†,‡,§] Li-Bo Han,[†,‡,§] Juan Wang,[†,‡,§] Yuan Yao,[†,‡,§] Hai-Yun Wang,[†,‡,§] Xiong-Ming Du,[||] Yuan-Ming Luo,[*,†] and Gui-Xian Xia[*,†,‡,§]

Institute of Microbiology, Chinese Academy of Sciences, Beijing 100101, State Key Laboratory of Plant Genomics, Beijing 100101, National Center for Plant Gene Research, Beijing 100101, and Institute of Cotton, Chinese Academy of Agricultural Sciences, Anyang 455112

Received October 28, 2009

Cotton fiber is an ideal model for studying plant cell elongation. To date, the underlying mechanisms controlling fiber elongation remain unclear due to their high complexity. In this study, a comparative proteomic analysis between a short-lint fiber mutant (*Ligon lintless*, Li_1) and its wild-type was performed to identify fiber elongation-related proteins. By 2-DE combined with local EST database-assisted MS/MS analysis, 81 differentially expressed proteins assigned to different functional categories were identified from Li_1 fibers, of which 54 were down-regulated and 27 were up-regulated. Several novel aspects regarding cotton fiber elongation can be illustrated from our data. First, over half of the down-regulated proteins were newly identified at the protein level, which is mainly involved in protein folding and stabilization, nucleocytoplasmic transport, signal transduction, and vesicular-mediated transport. Second, a number of cytoskeleton-related proteins showed a remarkable decrease in protein abundance in the Li_1 fibers. Accordingly, the architecture of actin cytoskeleton was severely deformed and the microtubule organization was moderately altered, accompanied with dramatic disruption of vesicle trafficking. Third, the expression of several proteins involved in unfolded protein response (UPR) was activated in Li_1 fibers, indicating that the deficiency of fiber cell elongation was related to ER stress. Collectively, these findings significantly advanced our understanding of the mechanisms associated with cotton fiber elongation.

Keywords: proteomics • cotton fiber • *Ligon* mutant • cytoskeleton • cell elongation

Introduction

Cotton fiber is a single and highly elongated epidermal cell of the cotton seed coat. Fiber development consists of four overlapping stages: initiation, elongation, secondary wall deposition, and maturation.[1] Fiber elongation begins on the day of anthesis and continues for 20−30 days, during which cotton fibers grow to 3−6 cm depending on the cultivars.[2] Due to the advantageous features such as extreme length and long duration of elongation, cotton fiber is regarded as a model system for studying the mechanisms controlling plant cell elongation.[3]

Significant progress has been made in large-scale identification of genes and proteins involved in fiber elongation during recent years. Through transcriptome analysis, Arpat et al. identified 2553 unique ESTs (uniESTs) from fiber cells of the diploid variety *Gossypium arboretum*,[4] and Shi et al. identified 778 uniESTs expressed preferentially or specifically during the elongation stage of fiber development in the tetroploid cotton variety *G. hirsutum*.[5] At protein level, Yang et al. studied the protein profiles in different stages of fiber development and identified 106 differently expressed proteins,[6] and Li et al. found 49 proteins accumulated specifically in elongating fiber cells by comparing the proteome profiles of a fuzzless-lintless mutant and its wild-type.[7] In addition to large-scale genes and proteins identification, a number of fiber elongation-related genes have been structurally or functionally characterized. Among them, a sucrose synthase gene (*Sus*), an actin gene (*GhACT1*), and a gene encoding a rate-limiting enzyme (GhDET2) in brassinosteroid (BR) biosynthesis were shown to be crucial for fiber elongation.[8−10] Although identification of these genes or proteins has made a substantial contribution to understanding the molecular basis of cotton fiber development, the underlying mechanisms that regulate fiber elongation are still unclear due to their high complexity.

The *Ligon lintless* 1 (Li_1) is a mutant of upland cotton (*G. hirsutum*) and possesses extremely shortened fibers as compared to the wild-type plant (6 mm vs 30 mm). It was originally discovered by Griffee and Ligon in 1929[11] and subsequently characterized by several studies, which revealed that: (1) Li_1 is a monogenic, dominant mutant with a defect in fiber elongation and plant growth; (2) the inhibition of Li_1 fiber elongation

* Authors for correspondence: Gui-Xian Xia and Yuan-Ming Luo Institute of Microbiology, Chinese Academy of Sciences, Beijing 100101, China. Telephone: +86 10 64845674, Fax: +86 10 64845674, E-mail: xiagx@im.ac.cn, luoym@im.ac.cn.
† Chinese Academy of Sciences.
‡ State Key Laboratory of Plant Genomics.
§ National Center for Plant Gene Research.
|| Chinese Academy of Agricultural Sciences.

10.1021/pr900975t

Table 1. Sequences of the Primers Used for Real-Time PCR Analysis

gene	accession no.	primers
PFN	EV489411	F 5′ ACCTTTCTGCCGCTGCTATCG 3′ R 5′ CGCCCAACCTCTCCACAACC 3′
TUB1	DT544715	F 5′ AAGGAAGCCGAGAATTGCGATTG 3′ R 5′ CGAGGGAATGGAATAAGGTTTACAGC 3′
RanBP1	CO131457	F 5′ GAGGAAGTCGCCGTTACCAC 3′ R 5′ TTTGTATCCTCCTTTGTTTCCGTTTC 3′
CaM	ES831951	F 5′ ATCTGAGACATATACTGACTAGCATCGG 3′ R 5′ AGAAAGAGTGTTACCATTAGTTCCAAAGG 3′
VIN	ES832477	F 5′ CGACATAGGCACCGCTACTCAG 3′ R 5′ CACCGTCCTCCCTCCTTCTCC 3′
HSP90	ES821537	F 5′ ATTCCGATGACTTGCCGCTTAAC 3′ R 5′ GCTTCTTGCCGTTGTATCCCTTC 3′
SNF7	DW245123	F 5′ TGCCAAAGGGAGAAACAAGAGAG 3′ R 5′ CCAAGAGGAGTTGACAGTGCTTC 3′
GLP	EV485102	F 5′ TCCGTACCGCAGGCAACAC 3′ R 5′ GTTCATTCAATAAGTCAGTCGCAAGTC 3′
CRT	ES850077	F 5′ TGAAGAAGCAGAGAAAGAACGAAGAG 3′ R 5′ ACGACGACAACAATGAGAACAACC 3′
His3	AF024716	F 5′ GCCAAGCGTGTCACAATTATGC 3′ R 5′ ACATCACATTGAACCTACCACTACC 3′

appeared at ~5−7 DPA (days post anthesis) and the fiber cells preterminated their growth among 13 DPA; (3) as little difference was found between the wild-type and Li_1 fibers during the initiation stage of fiber development, the elongation factors may account for the difference in cell length of the two types of fibers.[12−15] A striking feature of the Li_1 mutant is that while the elongation of the lint fibers was strictly impaired, the growth of the fuzz (a type of short fibers coexisting on the ovules with lint fibers) was not affected.[16,17] Hence, the elongation defect of lint fibers can be studied independent of the fuzz fibers in Li_1 mutant. On the basis of these genetic and phenotypic traits, the Li_1 mutant can stand out from the limited number of fiber elongation mutants as a unique cotton plant material viable for studying fiber elongation.

In the present study, we attempted to use a proteomic approach to compare the protein profiles between the Li_1 mutant and its wild-type to reveal more functional proteins involved in fiber elongation. We successfully identified 81 fiber elongation-related proteins, including a large portion of newly identified proteins that are involved in different biological processes.

Materials and Methods

Plant Materials. *Ligon* mutant and its wild-type cotton plants were grown in greenhouse. Cotton bolls were tagged on the day of anthesis. The fresh cotton ovules with fibers were harvested at 6 and 12 DPA, and fibers were carefully stripped from the ovules. All materials were immediately frozen in liquid nitrogen and stored at −80 °C until use.

In Vitro Culture of Cotton Fibers and Treatment with HSP90-Specific Inhibitor. Cotton ovules were cultured *in vitro* following the protocol of Beasley and Ting.[18] Bolls on cotton plants were collected on 2 DPA and ovules were dissected from the ovaries and floated on the basal medium containing 5 μM indole-3-acetic acid and 0.5 μM gibberellic acid. Cultures were grown at 32 °C in the dark. For treatment of fibers with HSP90-specific inhibitor, radicicol (Sigma-Aldrich Corp, St. Louis, MO, USA) with concentrations 0.1 or 1 μM was added to the medium at 5 DPA and DMSO was added as a mock treatment. Ovules were collected at 12 DPA for fibers length measurement.

RNA Extraction and Real-Time PCR. Total RNA of cotton fibers was extracted by ultracentrifugation as previously described.[19] First-strand cDNA was synthesized from 4 μg of total RNA using the SuperScript III first-strand synthesis system for reverse transcription (Invitrogen, Carlsbad, CA). Aliquots of the RT product were used for quantitative real-time PCR (qRT-PCR). Cotton *histone3* gene was used as an internal control. QRT-PCR assays were performed by using SYBR Green Realtime PCR Master Mix (Toyobo, Osaka, Japan) and DNA Engine Opticon 2 Real-Time PCR Detection System (MJ research). All reactions were performed in triplicate. Primers used in this study were shown in Table 1.

Protein Extraction and Quantification. Cotton fiber proteins were extracted according to a published protocol with minor modification.[20] Briefly, fibers were stripped from the ovules and ground with 10% (w/w) PVPP and 10% (w/w) quartz sand in liquid nitrogen. The powder was extracted with 10% (w/v) TCA and 0.07% (v/v) 2-mercaptoethanol (2-ME) in acetone for 1 h at −20 °C, and subsequently centrifuged at 20 000*g* for 20 min at 4 °C. The pellet was washed twice with cold (−20 °C) acetone containing 0.07% 2-ME and dried in air on ice, followed by a second-round extraction with buffer containing 30% sucrose, 0.1 M Tris-HCl (pH 8.8), 2% SDS, 2 mM PMSF and 0.07% 2-ME. An equal volume of phenol saturated with Tris-HCl (pH 8.6) was added to the extract and the mixture was vortexed for 1 h and then centrifuged at 20 000*g* for 20 min at room temperature. The upper phenolic phase was removed to a new tube and the proteins were precipitated with five volumes of 0.1 M ammonium acetate in methanol at −20 °C overnight. After centrifugation at 20 000*g* for 20 min at 4 °C, the pellet was rinsed twice with ice-cold 0.1 M ammonium acetate in methanol and twice with ice-cold 80% acetone. The air-dried pellet was resuspended in isoelectric focusing (IEF) buffer containing 7 M urea, 2 M thiourea, 4% CHAPS, 40 mM DTT, 2% (v/v) IPG buffer (pH 4−7). Protein concentration was determined with 2-D Quant kit (GE Healthcare Life Sciences, NJ, USA). The supernatant containing the soluble protein fraction was immediately subjected to 2-DE for protein separation.

2-DE and Image Analysis. Total proteins (1 mg) were loaded onto 24 cm IPG (pH 4−7) strips (GE Healthcare Life Science)

with rehydration buffer containing 7 M urea, 2 M thiourea, 4% CHAPS, 40 mM DTT and 0.5% (v/v) IPG buffer (pH 4−7). The IPG trips were rehydrated for 12 h at 30 V. IEF was performed with the IPGphor III system (GE Healthcare Life Science) at total voltage-hours of 80 kVh using the following conditions: 1 h at 100 V, 1 h at 300 V, 1 h at 500 V, 1 h at 1000 V, gradient to 4000 V in 1 h, gradient to 8000 V in 1 h and finally 10 h at 8000 V. The strips were incubated in equilibration buffer containing 1% DTT and 2.5% iodoacetamide. Proteins in the equilibrated strips were then separated in 12.5% denatured SDS polyacrylamide (SDS-PAGE) gels. After electrophoresis, proteins were stained by Coomassie Brilliant Blue (50% methanol, 0.15% CBB G-250 and 0.75% acetic acid) for 48 h on an orbital shaker. The stained gels were imaged using the ImageScanner III scanner (GE Healthcare Life Science) and image analysis was processed with ImageMaster 2D Platinum software (version 6.0, GE Healthcare Life Science). Detection and match of the protein spots were carried out by an automatic analysis mode, followed by visual re-evaluation. The detected protein spots were quantified using the percent volume criterion and the spots that showed a change of more than 1.8-fold between wild-type and Li_1 mutant were selected. For statistical analysis, a significant difference was defined at a level of p-value <0.05 based on Student's two-tailed t test for unpaired means.

MALDI-TOF MS and MS/MS Analyses. Protein spots were excised from gels and digested in-gel using trypsin. The resulting peptide mixtures were dissolved in 0.7 μL of CHCA matrix solution (5 mg/mL CHCA in 50% ACN/0.1% TFA) and spotted onto a freshly cleaned target plate. After air drying, the crystallized spots were processed with a MALDI-TOF/TOF mass spectrometer (4700 Proteomics Analyzer, Applied Biosystems, Framingham, MA). All mass spectra were recorded in a reflector mode within a mass range from 900 to 3700 Da, using a laser operated at a 200 Hz repetition rate with wavelength of 355 nm. The accelerated voltage was 2 kV. Internal calibration of the instrument was automatically performed by a peptide standard Kit (Applied Biosystems) that included des-Arg1-bradykinin (m/z 904), angiotensin I (m/z 1296), Glu1-fibrinopeptide B (m/z 1570), ACTH (1−17, m/z 2903), ACTH (18−39, m/z 2,65) and ACTH (7−38, m/z 3657). The MS/MS mass spectra were acquired by the data-dependent acquisition method with the 10 strongest precursors selected from one MS scan. All the MS/MS spectra resulted from accumulation of at least 3000 laser spots. The combined MS and MS/MS peak lists were searched using the GPS Explorer software version 3.5 (Applied Biosytems) against a *Gossypium* peptide sequence database created from *Gossypium* EST database (376 100 entries). Search parameters were as follows: trypsin digestion with one missed cleavage, variable modifications (oxidation of methionine and cabamidomethylation of cysteine), and mass tolerance 0.2 Da for MS and MS/MS data. Furthermore, the peaks at m/z 2163.05 and 2273.15 due to autolysis of trypsin were excluded from the peak lists. In all protein identifications, Peptide Mass Fingerprint or MS/MS, the probability scores were greater than the score fixed as significant with a p-value <0.05.

Annotation of EST Database. A total of 376 100 EST sequences for *Gossypium* species (AS, all sequences) were downloaded in January 2009 as FASTA format from the National Center for Biotechnology Information (NCBI, http://www.ncbi.nlm.nih.gov). The annotation of EST database was carried out as previously described in order to produce peptide sequence database that would be used for database search in protein identification.[21] Coding Sequence (CDS) was identified by a program based on "GetORF", which takes the longest CDS in all 6 translated frames as potential gene. A BLASTX analysis was subsequently performed against the NCBInr database in order to identify the best frame of translation and to confirm the protein. Functional categories of the identified proteins were assigned by Gene Ontology tool (http://www.geneontology.org).

Western Blotting Analysis. Proteins were extracted from 12 DPA fibers in 50 mM phosphate buffer (pH 7.2). Protein concentration of the supernatant was determined by the Bradford assay.[22] Ten micrograms of proteins were separated in 12% SDS-PAGE gel and transferred to a nitrocellulose membrane (Amersham Biosciences). The filter was blocked overnight with 5% (w/v) milk powder in 20 mM Tris-HCl (pH 7.5), 0.9% (w/v) NaCl, and then incubated with the polyclonal antibodies raised against human HSP90 (1:1000) or mouse α-tubulin (1:1000) for 1 h at 37 °C. After three washes, the filters were incubated for 1 h with anti-rabbit or anti-mouse IgG AP-conjugated antibody (1:5000) (Promega, Madison, WI), and the protein signals were detected by using a chemiluminescent kit (Promega).

Staining of Filamentous Actin. Filamentous actin (F-actin) staining was performed according to Seagull with slight modifications.[23] *In vitro* cultured 12 DPA fibers attached on ovules were incubated for 10 min in 0.66 mM Alexa Fluor 488 phalloidin (Molecular Probe) in PBS buffer (pH 7.0) containing 0.1 M PIPES, 0.05% Triton X-100, 1 mM $MgCl_2$, 3 mM DTT, 0.3 mM PMSF, 5 mM EGTA and 1% glutaraldehyde. After being rinsed in PBS buffer, fibers were carefully cut off from the ovules on glass slides. Actin structure was visualized using a Leica TCS SP5 spectral confocal microscope (Leica Microsystems, Heidelberg, Germany). Alexa-Fluor label was excited at 488 nm with emission from 520 nm.

Immuno-Labeling of Microtubules. Immunolabeling of microtubules was performed according to Preuss et al.[24] Briefly, *in vitro* cultured 12 DPA fibers were fixed in PEM buffer (50 mM PIPES, 5 mM EGTA and 1 mM $MgSO_4$, pH 6.9) containing 4% (w/v) paraformaldehyde, 0.1% Triton X-100, and 0.3 M mannitol for 10 min under a vacuum and 40 min at room temperature. Ovules were rinsed three times with PEM buffer for 10 min each time. Fibers were cut off from the ovules with a scalpel and attached to slides coated with poly-L-lysine (Sigma-Aldrich Corp). The fibers were incubated with 1% (w/v) Cellulase R-10 (Yakult, Japan) and 0.1% (w/v) Pectolyase Y-23 (Kikkoman, Japan) in PEM buffer containing 0.3 M mannitol and 1 mM PMSF for 10−20 min at room temperature, and then washed in PBS buffer (pH 7.0) three times for 10 min each time. The slides were preincubated in the buffer containing 1% (w/v) BSA in PBS buffer and then incubated with mouse monoclonal anti-α-tubulin antibody (1:1000) at 4 °C overnight. The specimens were then washed three times (10 min each time) in PBS buffer and incubated for 1 h with FITC-labeled goat anti-mouse secondary antibody (1:200). Slides with fiber cells were carefully washed in PBS buffer and sealed with nail polish before observation.

Microtubules were visualized using a Leica TCS SP5 spectral confocal microscope. The FITC Fluorlabel was excited at 488 nm with emission from 520 nm.

Vesicle Staining. Green fluorescent FM4−64 dye (Molecular Probes) was used to visualize the vesicles in fiber cells. *In vitro* cultured fibers (12 DPA) were incubated with FM4−64 dye in a final concentration of 5 μg/mL for 5−10 min. After rinsing

briefly with PBS buffer (pH 7.0), FM4−64 fluorescence was detected using a Leica TCS SP5 spectral confocal microscope. The FM4−64 fluorescence was excited at 543 nm with emission from 640 nm.

Microscopy Analyses. For scanning electron microscopy (SEM) analysis, bolls were harvested from the cotton plant grown in green house at 12 DPA and fibers were fixed in 2.5% glutaraldehyde in phosphate buffer (50 mM, pH 7.2) at 4 °C overnight. After dehydration in gradient ethanol series, the samples were treated with 100% isopentyl acetate at 4 °C overnight. The materials were then dried using a critical point dryer (model HCP-2, Hitachi, Tokyo, Japan), sputter coated with gold in an E-1010 ion sputter (Hitachi) and visualized under a scanning electron microscope (Quanta200, FEI Company, Netherlands).

For transmission electron microscopy (TEM) analysis, cotton fibers (12 DPA, grown in green house) were fixed in 2.5% glutaraldehyde in phosphate buffer (50 mM, pH 7.2) at 4 °C overnight. After three washes, the fibers were incubated in 1% osmium tetraoxide for 4 h at room temperature. The specimens were washed for three times and dehydrated in a series of ethanol and epoxy ethane, and then embedded in Epon 812 resin for 48 h at 60 °C. The middle parts of the fibers were cut into thin sections (50 nm) with an LKB III Ultratome, stained with uranyl acetate followed by lead citrate, then examined and photographed under a JEM-1400 electron microscope (JEDL LTD, Japan).

Results

Morphology of the *Li*$_1$ Mutant. The morphology of the short-lint fiber mutant *Li*$_1$ has been reported by several previous studies.[13−15] While the dominant homozygote (*Li*$_1$*Li*$_1$) was lethal, the heterozygote (*Li*$_1$*li*$_1$, referred to as *Li*$_1$ throughout the text) showed pleiotropic morphology changes such as smaller size and distorted growth in leaves and stems (Figure 1A). The most prominent feature of *Li*$_1$ cotton is that it possesses extremely shortened fiber cells. In contrast to the wild-type fibers that have a cell length of ~30 mm, the mutant fibers are as short as ~6 mm (Figure 1B, upper panel). To better characterize the morphological changes of the mutant fibers, we further examined the ultrastructure and the cell surface morphology of the 12 DPA *Li*$_1$ fibers by transmitting electron microscopy (TEM) and scanning electron microscopy (SEM). The TEM images revealed a remarkable variation in the primary wall structure of the *Li*$_1$ fiber. A compact cuticle layer with highly electron-dense deposits was visible at the outmost periphery of the cell wall of the *Li*$_1$ fiber, and the overall primary wall showed higher electron density than the wild-type control as well (Figure 1C). SEM analysis indicated that the mutant fiber cell displayed a rough and crinkly surface, forming a sharp contrast to a smooth surface of the wild-type fiber, as shown in Figure 1D.

Analysis of Proteome Profiles and Identification of Differential Proteins. As represented in previous reports,[12,13] *Li*$_1$ fibers preterminated the elongation among 13 DPA during fiber development, we therefore chose the fibers at 12 DPA (Figure 1B, lower panel) for proteomic analysis. Total soluble proteins were extracted from three biological replicates of the wild-type and *Li*$_1$ fibers and analyzed by 2-DE. Each sample was analyzed in triplicate and the 2-DE maps of the wild-type and *Li*$_1$ fibers are shown in Figure 2. A total of 1200 ± 50 spots were found on both CBB stained gels (Figure 2A, B). Protein amounts of the detected spots on normalized gels were quantified with

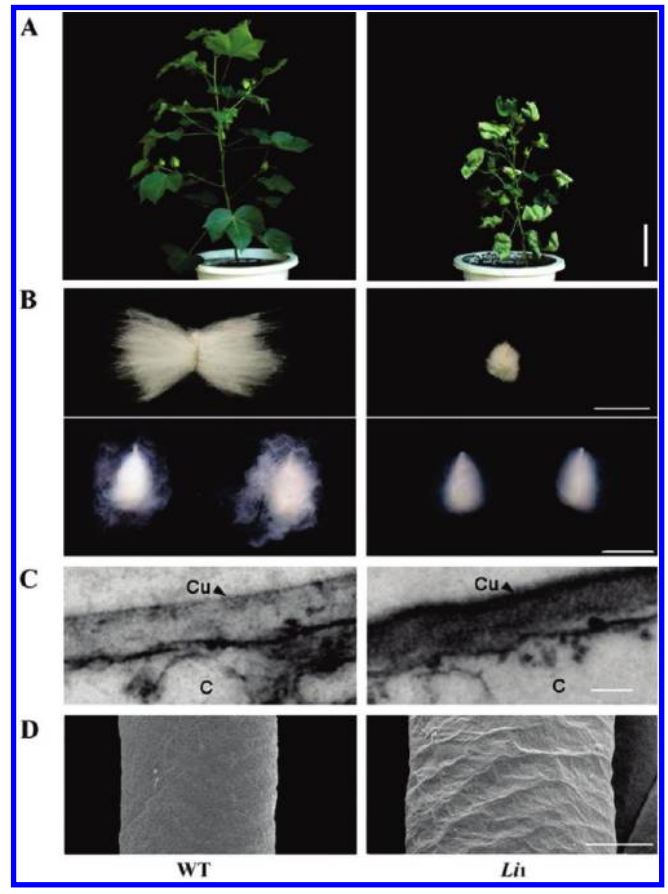

Figure 1. Morphology of wild-type (WT, left) and *Li*$_1$ mutant (*Li*$_1$, right) cotton. (A) Adult cotton plants of wild-type and *Li*$_1$ mutant. Bar = 10 cm. (B) Ovules attached with fibers. Upper panel: mature fibers, Bar = 1.5 cm; lower panel: 12 DPA fibers, Bar = 1 cm. (C) TEM images of cell wall of wild-type and *Li*$_1$ fibers at 12 DPA (c, cytoplasm; cu, cuticle,). Bar = 0.1 μm (D) SEM images of cell wall surface of wild-type and *Li*$_1$ fibers at 12 DPA, Bar = 10 μm.

ImageMaster 2D Platinum software and the average intensity of the spots was measured. About one hundred differentially expressed protein spots (p-value < 0.05) were detected by image analysis. Of which, 81 spots showed more than 1.8-fold changes in the relative abundance between wild-type and *Li*$_1$ fibers and were selected for further analysis. Among these protein spots, 54 were found on the wild-type map while 27 were detected on *Li*$_1$ map. Figure 2C and D show the representative features of the protein spots.

To gain a more complete picture on the proteins associated with deficient elongation of the *Li*$_1$ fibers, proteomic analysis was also performed with the fibers of 6 DPA when the inhibition of *Li*$_1$ fiber elongation started to be observable. No significant difference in the protein expression profiles was found between the wild-type and *Li*$_1$ fibers at 6 DPA (data not shown) as compared to 12 DPA, indicating that differential protein expression occurred mainly after 6 DPA in the *Li*$_1$ fibers.

Construction of EST Database of *Gossypium* and Functional Annotation. The selected protein spots were excised from gels, in-gel digested with trypsin and subjected to MALDI-TOF/TOF MS analysis. Initially, only 50−60% protein spots among the ultimately confirmed proteins were exactly identified by searching the NCBInr database and online EST database with MS combined with MS/MS spectra, a customarily employed technological routine. There were no matches of a

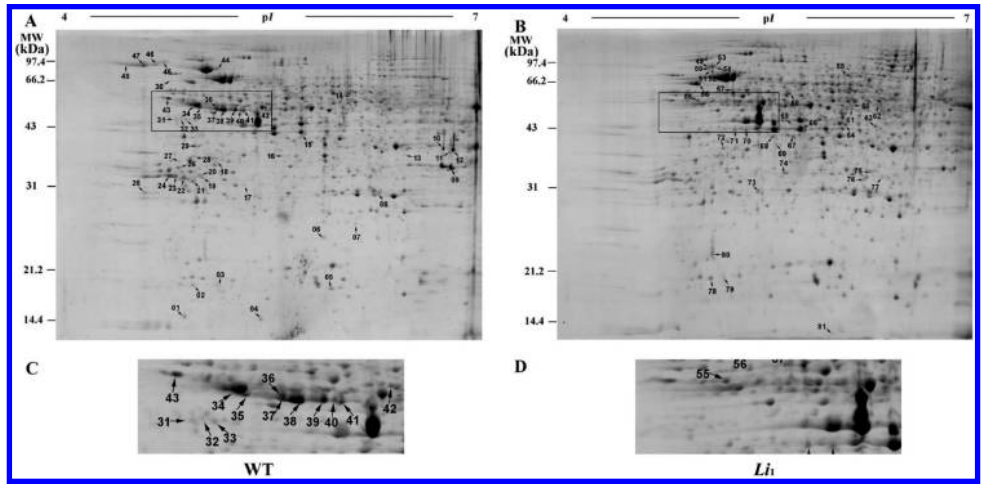

Figure 2. 2-DE map of total proteins from 12 DPA cotton fibers. (A) Wild-type. (B) Li_1 mutant. As spots 49−54 are too closely located in 2-DE map of wild-type, they are marked in Li_1 mutant map to distinguish individuals. The framed regions are enlarged to clearly show the spot numbers of wild-type (C) and Li_1 (D).

considerable protein spots by searching against with these databases due to lack of the completely sequenced cotton genome. A specific local peptide sequence database corresponding to EST sequences of *Gossypium* species was therefore established by annotating approximately 376 000 EST sequences with GoPipe software.[21] All the obtained MS and MS/MS spectra were searched utilizing the GPS Explorer software version 3.5 (Applied Biosytems) against this established peptide sequence database. The availability of this database enabled us to acquire more protein spot matches, thereby significantly enhancing the efficiency and accuracy of identification. A BLASTX analysis was next performed on each EST sequence with the highest MASCOT score to confirm the protein spots. Tables 2 and 3 provide the accession numbers corresponding to the protein spots shown in Figure 2, the names of the putative proteins, species, the MASCOT score together with sequence coverage and the theoretical and observed MW/*p*I values. Some of the spots were identified as the same protein but displayed different *p*I and MW values. These proteins might represent different modifications of the same gene product or isoforms of the same protein family. Of the 81 identified proteins, 39 were previously reported to be related with cotton fiber development, while 42 proteins were newly identified at the protein level.

Proteins Differentially Expressed in Li_1 Fibers. The identified proteins were functionally categorized by the Gene Ontology Tool. The down-regulated proteins in the Li_1 fibers were classified into nine categories, mainly included cytoskeleton, nucleocytoplasmic transport, protein fate, signaling and metabolism subclasses (Figure 3A). Proteins up-regulated in the Li_1 fibers were assigned into five groups, implicated primarily in the stress response, unfolded protein response (UPR), and cellular metabolism (Figure 3B).

Two important aspects can be defined from the down-regulated proteins. (1) More than half of the proteins are newly identified. These proteins belong to several functional disciplines including molecular chaperon (HSP90 proteins and HSP70-interacting protein1), nucleocytoplasmic transport (Ran-binding proteins, Ran GTPase-activating protein and glycine-rich RNA-binding protein), cell expansion (vacuolar invertases) and vesicle transportation (vacuolar-sorting protein SNF7, γ-soluble nsf attachment protein and coatomer-like protein) (Table 2). (2) Among the 54 down-regulated proteins in the Li_1 fibers the cytoskeleton-related proteins accounted for 27% of the total proteins, consisting of five α-tubulin isoforms, two β-tubulin isoforms, five annexin isoforms, one tubulin folding cofactor A and one profilin. In addition to these newly identified proteins, a number of others proteins that were previously reported to be associated with cotton fiber development were also found to be suppressed in Li_1 fibers. These proteins are implicated principally in protein modification and proteolysis (proteasome subunit), signal transduction (calmodulin and 14-3-3 isoforms), cell wall biogenesis (UDP-glucose pyrophosphorylase and reversibly glycosylated polypeptide), and cellular metabolism (transaldolases, inorganic pyrophosphatase and phenylcoumaran benzylic ether reductase-like protein).

The proteins with enhanced expression in Li_1 fibers fall into three major groups. Among them, nine proteins were designated as members of stress responses, comprising polyphenol oxidase, nucleoredoxin, glutathione reductase, alcohol dehydrogenase, chloroplast stromal ascorbate peroxidase, germin-like protein isoforms and stress-related protein. Four proteins were assigned to be associated with unfolded proteins response, including protein disulfide isomerase isovarients and calreticulin. Additionally, expression of three protein elongation factors and several other proteins involved in cellular metabolism or energy production, including ketol-acid reductoisomerase, chloroplast β-ketoacyl-ACP synthase precursor, glutamine synthetase, flavanone 3-hydroxylase, dihydrodipicolinate synthase, diaminopimelate epimerase, triosephosphate isomerase, ATP synthase D chain and succinyl CoA ligase β subunits, were enhanced in Li_1 fibers as well.

Verification of Differential Expression via Western Blotting Analysis and Real-Time PCR. Western blotting analysis was conducted to verify the differences of the expression levels between the proteins from wild-type and the Li_1 mutant. Tubulin and HSP90 proteins were taken as examples for the test. As shown in Figure 4A, both tubulin and HSP90 expression was significantly suppressed in Li_1 fibers as compared to the wild-type control. This result was in agreement with those of the 2-DE shown in Figure 2A.

Real-time PCR analysis was carried out for 9 proteins to examine if the expression changes were consistent at the mRNA and protein levels. Concordant differential expression at the mRNA level was observed with at least half of the analyzed

Table 2. Down-Regulated Proteins in Li_1 Identified by MS/MS

spot ID	protein name	NCBI acc. no.	species	mascot Score	peptides matched	sequence coverage	theoretical MW (kDa)/p*I*	observed MW (kDa)/p*I*	ratio[a]
			Cytoskeleton						
34	tubulin beta-1	DT544715	*Gossypium hirsutum*	588	23	57%	50.00/4.67	51.20/4.96	4.85[b]
36	alpha-tubulin	ES828302	*Gossypium hirsutum*	401	26	45%	49.70/4.91	49.10/5.13	4.75[b]
38	alpha-tubulin	DT571427	*Gossypium hirsutum*	547	27	59%	49.57/4.85	48.33/5.18	10.09[b]
39	alpha-tubulin	ES807127	*Gossypium hirsutum*	479	25	40%	49.69/4.91	48.68/5.26	3.87[b]
41	alpha-tubulin	ES807127	*Gossypium hirsutum*	264	21	37%	49.69/4.91	48.68/5.32	9.34[b]
35	beta-tubulin 1	CO107623	*Gossypium raimondii*	561	25	48%	50.00/4.67	49.00/5.0	ND
37	alpha tubulin	EE592712	*Gossypium barbadense*	432	31	50%	49.58/4.90	48.50/5.11	ND
40	alpha-tubulin	ES828302	*Gossypium hirsutum*	328	27	40%	49.70/4.91	48.66/5.27	4.01
03	tubulin folding cofactor A	DW516203	*Gossypium hirsutum*	115	13	81%	12.82/4.87	18.33/5.13	ND
04	profilin	EV489411	*Gossypium hirsutum*	321	9	42%	14.25/5.48	14.16/5.43	4.09[b]
13	annexin	ES793672	*Gossypium hirsutum*	244	28	58%	36.05/6.45	37.33/6.46	ND
10	annexin	CO129429	*Gossypium raimondii*	609	31	63%	36.05/6.45	40.23/6.75	4.9[b]
12	annexin	ES795476	*Gossypium hirsutum*	234	12	56%	36.05/6.45	39.50/6.80	3.62
09	annexin	ES795476	*Gossypium hirsutum*	259	12	64%	36.05/6.45	35.13/6.80	3.13
11	annexin	ES804937	*Gossypium hirsutum*	466	34	59%	36.05/6.45	38.33/6.80	1.89
			Protein folding and stabilization						
49	HSP90	ES810068	*Gossypium hirsutum*	468	28	37%	80.15/4.90	91.0/5.01	7.25[c]
50	HSP90	ES848757	*Gossypium hirsutum*	518	22	55%	88.0/5.01	91.00/5.01	7.25[c]
51	HSP90	ES821537	*Gossypium hirsutum*	293	25	54%	79.68/4,97	91.00/5.01	7.25[c]
52	HSP90	ES828488	*Gossypium hirsutum*	502	27	57%	88.0/5.04	88.00/5.01	7.25[c]
53	HSP90	ES837858	*Gossypium hirsutum*	226	25	54%	80.20/4.89	88.00/5.01	7.25[c]
54	HSP90	ES795715	*Gossypium hirsutum*	329	19	41%	89.0/5.07	87.00/5.01	7.25[c]
45	HSP90	ES797743	*Gossypium hirsutum*	86	13	34%	90.00/4.85	101.50/4.71	ND
44	HSP90	EV491935	*Gossypium hirsutum*	104	20	68%	80.77/4.99	94.66/5.11	ND
42	Hsp70-interacting protein 1	DT564504	*Gossypium hirsutum*	190	21	47%	44.94/4.84	51.50/5.46	ND
			Nucleocytoplasmic transport						
26	Ran-binding protein 1	CO131457	*Gossypium raimondii*	86	9	37%	24.12/4.58	35.33/4.82	3.86[b]
22	Ran-binding protein 1	DN757992	*Gossypium hirsutum*	165	10	47%	24.12/4.58	33.33/4.85	1.95
19	Ran-binding protein 1	DT558543	*Gossypium hirsutum*	219	13	44%	24.12/4.58	33.33/5.0	ND
20	Ran-binding protein 1	ES822775	*Gossypium hirsutum*	216	16	60%	24.12/4.58	34.3/4.97	2.39
21	Ran-binding protein 1	DN757955	*Gossypium hirsutum*	134	11	37%	24.12/4.58	32.16/4.93	2.67
30	Ran GTPase-activating protein	ES830968	*Gossypium hirsutum*	95	3	11%	58.02/4.48	65.00/4.77	ND
05	glycine-rich RNA-binding protein	DW231397	*Gossypium hirsutum*	323	15	70%	16.51/8.12	17.16/5.88	1.92
			Vesicle-mediated transport						
29	vacuolar-sorting protein SNF7	DW245123	*Gossypium hirsutum*	314	17	38%	24.36/4.71	39.00/5.97	3.15[b]
18	gamma-soluble nsf attachment protein	CO102209	*Gossypium raimondii*	110	10	29%	32.36/4.73	36.16/5.11	2.62[b]
17	coatomer-like protein	ES804905	*Gossypium hirsutum*	176	12	26%	32.31/5.40	32.16/5.30	2.53[b]
			Signal transduction						
25	14-3-3 protein	CO074226	*Gossypium raimondii*	648	22	43%	29.23/4.64	31.00/4.63	3.34
24	14-3-3 protein	DT557996	*Gossypium hirsutum*	76	5	30%	29.23/4.64	33.33/4.76	2.67
23	14-3-3 protein	BM359797	*Gossypium arboreum*	78	3	16%	29.23/4.64	33.33/4.80	3.39
27	14-3-3 protein	DW485067	*Gossypium hirsutum*	190	16	38%	29.23/4.64	36.33/4.83	ND
01	calmodulin	ES831951	*Gossypium hirsutum*	447	30	86%	16.51/4.64	14.00/4.85	5.08[b]
			Metabolism						
08	inorganic pyrophosphatase	DW484151	*Gossypium hirsutum*	96	11	31%	24.57/6.08	31.33/6.27	ND
07	glycolipid transfer protein	DT461234	*Gossypium hirsutum*	152	18	64%	22.54/6.49	27.33/6.10	1.88[b]
31	transaldolase	ES811387	*Gossypium hirsutum*	501	15	38%	47.81/5.46	50.33/4.81	2.44
33	transaldolase	DW225572	*Gossypium hirsutum*	137	14	55%	47.81/5.46	49.66/4.88	2.37[b]
32	transaldolase	ES811387	*Gossypium hirsutum*	359	23	64%	47.81/5.46	50.66/4.84	2.34[b]
46	vacuolar invertase	ES832477	*Gossypium hirsutum*	368	10	21%	71.82/4.69	92.00/4.62	ND
47	vacuolar invertase	ES832477	*Gossypium hirsutum*	311	11	24%	71.82/4.69	92.00/4.59	ND
48	vacuolar invertase	DT049468	*Gossypium hirsutum*	308	9	48%	71.82/4.69	92.00/4.44	ND
16	phenylcoumaran benzylic ether reductase-like protein	DW226959	*Gossypium hirsutum*	137	12	51%	33.79/5.92	39.21/5.57	ND
			Cell wall related proteins						
15	reversibly glycosylated polypeptide RGP	DT543039	*Gossypium hirsutum*	317	21	46%	40.85/6.21	41.66/5.70	2.26[b]
14	UDP-glucose pyrophosphorylase	EV482616	*Gossypium hirsutum*	204	12	40%	52.06/7.0	56.00/6.06	2.30[b]
			Protein modification and proteolysis						
02	small ubiquitin-like modifier 1(SUM1)	ES819189	*Gossypium hirsutum*	85	3	25%	10.97/4.79	19.00/4.93	2.07
28	proteasome subunit alpha type	DT549128	*Gossypium hirsutum*	375	18	53%	30.37/4.79	37.25/4.94	3.66
			Unclassified proteins						
43	hypothetical protein	DW008228	*Gossypium hirsutum*	650	25	68%	67.23/4.65	68.33/4.75	2.94[b]
06	hypothetical protein	DT459771	*Gossypium hirsutum*	164	10	37%	18.72/5.94	24.83/5.87	2[b]

[a] ND, not detectable in the 2-DE maps of wild-type or Li_1 mutant; Statistical significance was determined using Student's two-tailed *t* test for unpaired means. $P < 0.05$. [b] $P < 0.01$. [c] As spots 49−54 are too closely located in the 2-DE map of the wild-type, their protein abundance was quantified as one spot.

Table 3. Up-Regulated Proteins in Li_1 Identified by MS/MS

spot ID	protein name	NCBI acc. no.	species	Mascot score	peptides matched	sequence coverage	theoretical MW (kDa)/p*I*	observed MW (kDa)/p*I*	ratio[a]
			Stress responses						
59	polyphenol oxidase	DT570918	*Gossypium hirsutum*	503	25	67%	66.31/6.87	81.00/6.03	1.93
56	nucleoredoxin	DT545072	*Gossypium hirsutum*	197	21	55%	78.03/5.85	79.67/4.94	2.46
62	glutathione reductase	DT546041	*Gossypium hirsutum*	448	21	70%	53.81/5.75	64.20/6.26	2.31
64	alcohol dehydrogenase	ES849354	*Gossypium hirsutum*	631	30	63%	41.09/5.82	45.00/6.02	1.95[b]
75	chloroplast stromal ascorbate peroxidase	DT549779	*Gossypium hirsutum*	501	28	61%	39.63/7.35	34.16/6.22	2.68[b]
80	germin-like protein	EV485102	*Gossypium hirsutum*	396	17	77%	21.71/4.86	23.00/5.02	5.57[b]
79	germin-like protein	EV487732	*Gossypium hirsutum*	192	11	46%	21.71/4.86	20.50/5.13	ND
81	stable protein 1-related	DT052785	*Gossypium hirsutum*	68	2	14%	12.57/4.91	11.83/5.94	3.08
76	stress related protein	EV484202	*Gossypium hirsutum*	280	13	41%	27.54/5.96	32.66/6.17	3.22
			ER unfolded protein response						
57	protein disulfide isomerase	ES813734	*Gossypium hirsutum*	234	23	65%	55.53/4.83	57.66/5.19	2.04
67	protein disulfide isomerase	DT568576	*Gossypium hirsutum*	481	21	61%	39.40/5.66	40.83/5.64	1.88
55	protein disulfide isomerase	ES791121	*Gossypium hirsutum*	296	25	60%	55.56/4.85	53.20/4.92	2.66
60	calreticulin	ES850077	*Gossypium hirsutum*	246	13	57%	50.57/6.84	49.00/6.06	2.05
			Metabolism/Energy						
58	ketol-acid reductoisomerase	AI729872	*Gossypium hirsutum*	144	5	31%	63.92/6.82	70.66/5.62	2.2
61	chloroplast beta-ketoacyl-ACP synthase precursor	ES841459	*Gossypium hirsutum*	105	14	36%	50.00/7.85	53.00/6.06	2.09[b]
66	glutamine synthetase	ES817221	*Gossypium hirsutum*	481	20	44%	39.17/5.57	42.83/5.69	2[b]
68	flavanone 3-hydroxylase	DT554504	*Gossypium hirsutum*	458	29	77%	41.040/5.31	40.30/5.49	1.88[b]
69	dihydrodipicolinate synthase	ES825349	*Gossypium hirsutum*	99	9	30%	40.34/6.55	39.16/5.52	2.08[b]
72	diaminopimelate epimerase	DW234018	*Gossypium hirsutum*	483	25	61%	40.10/6.34	38.50/5.11	2.03
73	triosephosphate isomerase	ES805129	*Gossypium hirsutum*	587	25	64%	27.44/6.06	30.33/5.38	2.54[b]
78	ATP synthase D chain	ES828036	*Gossypium hirsutum*	250	19	77%	19.74/5.26	20.16/5.01	2.19
70	succinyl CoA ligase beta subunit	ES824252	*Gossypium hirsutum*	281	29	50%	44.83/5.93	42.16/5.29	3.21
71	succinyl-CoA ligase beta subunit	CO126388	*Gossypium raimondii*	165	26	60%	44.83/5.93	42.50/5.20	2.35[b]
			Protein biosynthesis						
74	eukaryotic translation elongation factor	ES815260	*Gossypium hirsutum*	296	26	51%	94.02/5.98	33.50/5.59	2.47[b]
63	Elongation factor Tu	CO130623	*Gossypium raimondii*	229	15	51%	49.03/6.92	44.50/6.25	1.87
77	eukaryotic translation elongation factor	ES808655	*Gossypium hirsutum*	226	17	62%	94.16/6.01	32.50/6.31	2.11[b]
			Unclassified proteins						
65	hypothetical protein	ES808433	*Gossypium hirsutum*	83	10	29%	29.23/5.93	45.33/5.63	2.06

[a] ND, not detectable in the 2-DE maps of wild-type or Li_1 mutant; Statistical significance was determined using Student's two-tailed *t* test for unpaired means. $P < 0.05$. [b] $P < 0.01$. [c] As spots 49−54 are too closely located in 2-DE map of wild-type, their protein abundance was quantified as one spot.

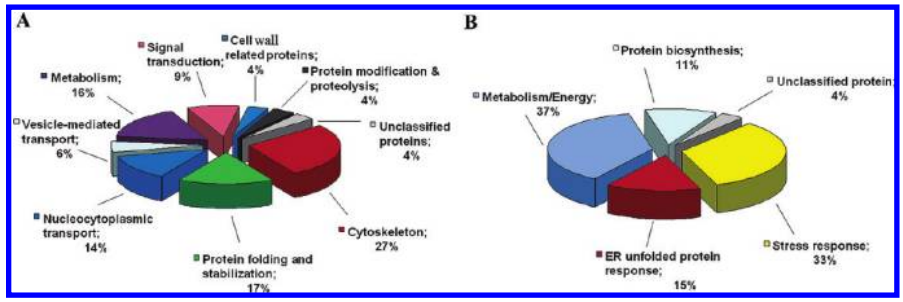

Figure 3. Functional categorization of identified proteins. (A) Down-regulated proteins in Li_1 fibers at 12 DPA. (B) Up-regulated proteins identified in Li_1 fibers at 12 DPA.

proteins, including tubulin β-1 (spot 34), profilin (spot 04), HSP90 (spot 51), Ran-binding protein 1 (spot 26), calmodulin (spot 01) and vacuolar invertase (spot 46) (Figure 4B). However, some of the tested proteins like vacuolar-sorting protein SNF7 (spot 29) and germin-like protein (spot 80) showed a weak protein-mRNA correlation and even a negative correlation as for the protein calreticulin (spot 60), suggesting a contribution of the post-transcriptional mechanisms such as messenger stability, post-transcriptional splicing, protein synthesis, post-translational modifications and degradation.[25,26] Such an inconsistence in the expression levels between mRNAs and proteins has been found by many other studies,[27−31] indicating that proteomic analysis is an indispensable approach for identification of the final products responsible for different cellular functions.

Changes in Cytoskeleton Organization and Vesicle Trafficking in the Li_1 Fibers. The fact that cytoskeleton-related proteins, such as tubulin, profilin and annexin occupied the largest fraction of the identified down-regulated proteins, attracted our particular attention. To see if these altered expression reflected defects in the cytoskeleton structures, we analyzed the cytoskeleton organization in the 12 DPA fiber cells. Not to our surprise, a dramatically aberrant actin organization was observed in the Li_1 fibers. While actin filaments formed cables that were arrayed parallel to the axis of the fiber elongation, F-actin organization was deformed dramatically in

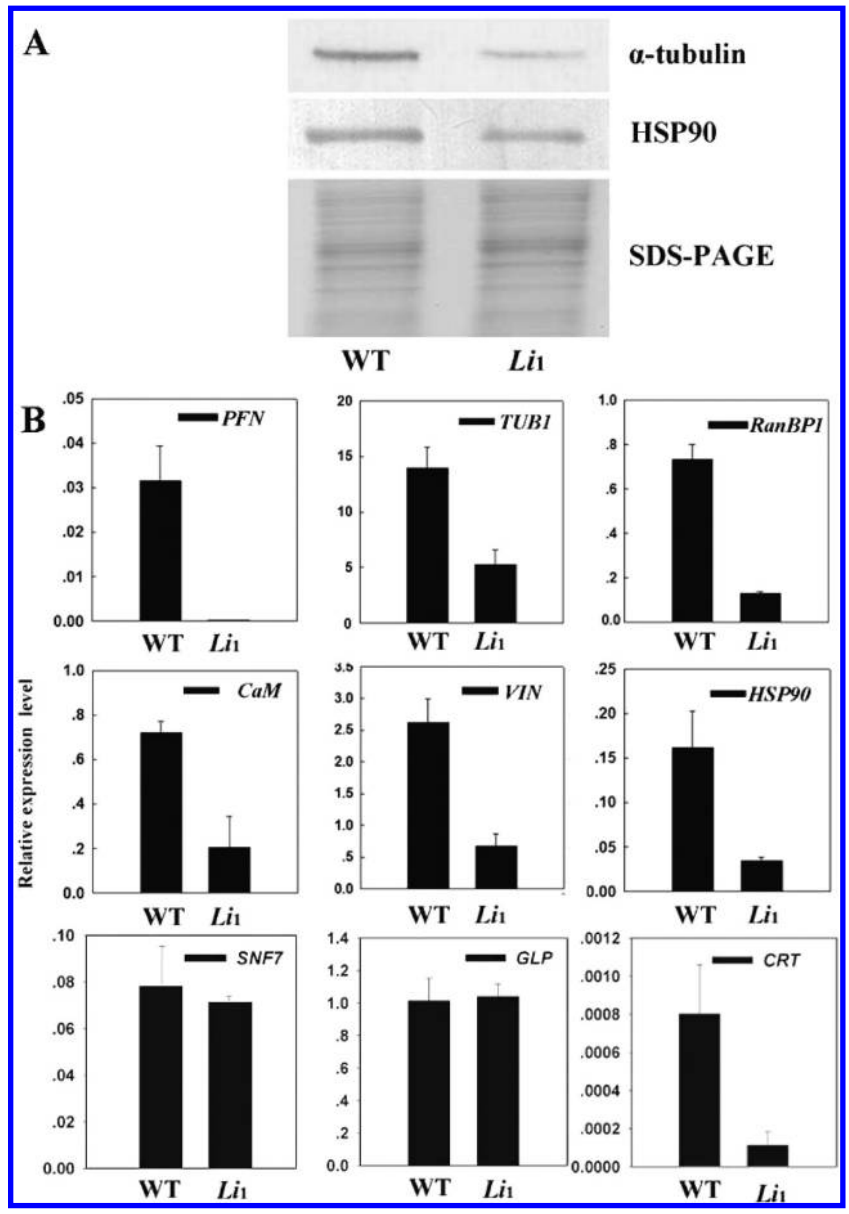

Figure 4. (A) Western blotting analysis of tublin and HSP90 expression in wild-type and Li_1 fibers at 12 DPA. (B) Real-time PCR analysis of the transcripts of selected proteins. PFN, profilin; TUB1, tubulin $\beta-1$; RanBP1, Ran-binding protein 1; CaM, calmodulin; VIN, vacuolar invertase; HSP90, heat shock protein 90; CRT, calreticulin; SNF7, vacuolar-sorting protein SNF7; GLP, germin-like protein.

the mutant fibers. The arrays of the F-actin filaments were shifted from longitudinal into horizontal or slanting orientations, and banked up into stacks or spiral bundles along the fiber cells (Figure 5A). In addition to actin cytoskeleton, the microtubules in the wild-type and Li_1 fibers were examined in parallel. As illustrated in Figure 5B, the microtubule organization in the 12 DPA Li_1 fibers appeared significantly different from those in the wild-type cell. While microtubule filaments were arranged into a horizontal orientation in the wild-type fibers, a portion of the microtubules were oriented in an oblique angle in the Li_1 fibers. Moreover, the microtubule filaments looked less dense in some regions of the Li_1 fibers than in the wild-type fibers. These results showed that the organizations of both types of cytoskeleton were aberrant in the Li_1 fiber, but the actin cytoskeleton was affected more severely.

Bright-field images of Li_1 fibers showed many regions with accumulated materials (Figure 5C). As it is known that cytoskeleton serves as tracks of intracellular transportation, we assumed that these dense materials might be the blocked vesicles due to the disrupted cytoskeleton structure. To see if this is true, the cellular vesicles in the fiber cells were labeled with FM4−64.[32] As shown in Figure 5C, while the vesicles were distributed uniformly in the wild-type fiber (upper panel), they were aggregated into patches in many regions along the Li_1 fiber that matched the dense materials observed under bright-filed microscope (lower panel), showing that the altered cytoskeleton organization may result in an impact on the vesicle trafficking in Li_1 fibers.

Inhibition of HSP90s Activities Affected Fiber Elongation. As 2-DE map showed dramatic decrease in the abundance of HSP90 proteins, the role of these proteins in fiber elongation was assessed by treating the *in vitro* cultured fibers with HSP90-specific inhibitor radicicol.[33] As shown in Figure 6A, fiber elongation was obviously inhibited after treatments with 0.1 or 1 μM radicicol. Compared to the mock-treated control fibers,

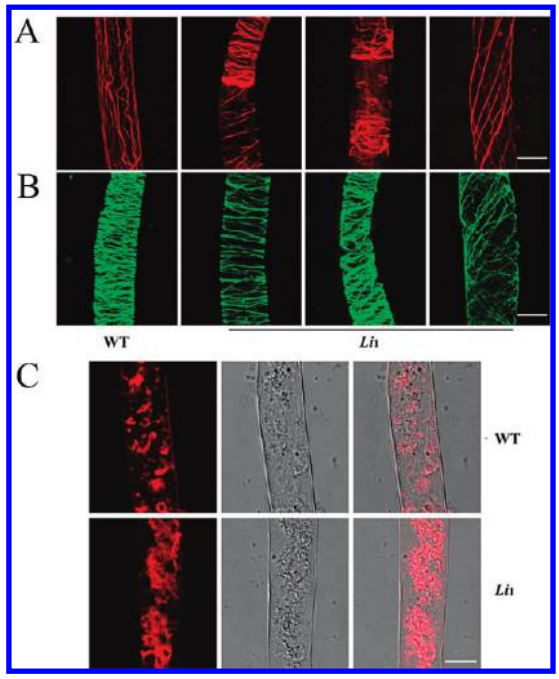

Figure 5. Structures of cytoskeleton and cellular vesicle distribution in wild-type and Li_1 fibers at 12 DPA. (A) Organization of F-actin cytoskeleton. Bar = 12.5 μm. (B) Organization of microtubule cytoskeleton. Bar = 12.5 μm. (C) Cellular vesicle labeled with FM4−64. upper panel, wild-type; lower panel, Li_1 mutant. Left, FM4−64 staining; middle, bright-field microscopy images; right, merged images. Bar = 12.5 μm.

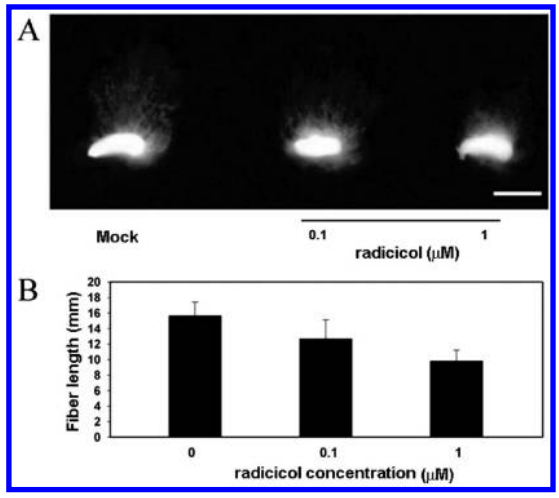

Figure 6. Effect of HSP90-specific inhibitor radicicol on the elongation of cultured wild-type fibers. (A) Mophology of 12DPA fibers grown in the medium with or without (mock) radiciol (bar = 0.5 cm). (B) Average fiber length measured at 12DPA after radicicol or mock (DMSO) treatments. Three independent experiments were conducted. Values are mean ± SD, n = 35.

the length of the treated fibers reduced about 37% (Figure 6B). This result indicated that proper HSP90 activities were required for fiber elongation, and meanwhile suggested that suppression of the HSP90 expression may be a causal factor for the deficient elongation of the Li_1 fibers.

Discussion

Newly Identified Proteins Associated with Fiber Elongation. One of the novel aspects of this research is the discovery of a number of proteins that were not identified by previous studies. These newly identified proteins include HSP90s, nucleocytoplasmic transporters, vesicle transporting proteins and vacuolar invertases etc. Identification of these proteins from the short-lint fiber mutant Li_1 added novel insights on the cellular processes important for cotton fiber elongation.

HSP70 proteins have been revealed to be possibly associated with fiber elongation.[6] In our work, another subclass of heat shock proteins, the HSP90, was found to be down-regulated in the Li_1 fibers. Accumulating evidence indicates that the HSP90 chaperon complex plays a critical role in plant development and response to external stimuli.[34] Suppression of these heat shock proteins in the Li_1 mutant fibers implied that proper folding of the proteins required for fiber elongation or its regulation may be affected by Li_1 mutation.

Ran-binding proteins play an essential role in nucleocytoplasmic transport in yeast and mammals.[35] Several studies indicated that they may perform similar functions in nuclear import and export in plants.[36−38] Among the down-regulated proteins in Li_1 fibers, there were five Ran-binding proteins (RanBP1 isovarients) and one Ran GTPase-activating protein. In addition, a glycine-rich RNA-binding protein participating in nucleocytoplasmic transporting of protein or RNA also exhibited down-regulated expression in Li_1 fibers. Suppression of these proteins suggests that the nucleocytoplasmic transport of certain proteins such as regulatory proteins may be affected in Li_1 fibers.

Other newly identified proteins include the vacuolar invertase that was known to participate in turgor-mediated cell elongation, and the proteins involved in vesicle transport etc. Down-regulation of these proteins in Li_1 fibers reflected their roles in the elongation of fiber cells.

Cytoskeleton Plays a Critical Role in Cotton Fiber Elongation. Accumulating experimental data indicate that cytoskeleton plays an essential role in cotton fiber development. For example, it was shown that inhibition of an actin gene (*GhACT1*) expression resulted in terminated fiber elongation.[9] In this work we found that the actin organization was disrupted severely in Li_1 fibers. In accordance with this structural alteration, one profilin and five annexin isovarients were markedly down-regulated in the mutant. It is widely known that both profilin and annexin are important regulators of actin organization. Annexins can mediate the interation between the actin cytoskeleton and membranes.[39,40] Profilin functions in promoting actin polymerization, and suppressed expression of profilin resulted in disrupted actin organization in *Arabidopsis* cells.[41] As we did not find differential expression of the actin proteins in the Li_1 fibers by 2-DE and Western blotting analyses (data not shown), the strong decrease in the expression levels of profilin and annexin proteins may account for, at least partly, the deformation of the actin arrangements in the Li_1 fibers.

Microtubules consist of another important type of cytoskeleton. Expression of seven tubulin isoforms was suppressed in Li_1 fibers. Accordingly, alterations in the microtubule thickness and arrangement were observed in the mutant fiber cell, indicating that Li_1 mutation also affected microtubule organizations. Previously, through expression analysis, actin and microtubule cytoskeleton-related genes were frequently reported to be involved in fiber elongation.[6,42,43] Herein, the correlation between alteration of the cytoskeleton architectures and suppressed expression of the cytoskeletal proteins in the Li_1 mutant provides a more direct line of evidence to show the important role of cytoskeleton in fiber elongation.

A remarkable growth rate of cotton fiber requires an accelerated traffic of membrane vesicles and cell wall materials to the point of the deposition. We found that accompanying with the disorganization of cytoskeleton structures, the cellular vesicles were aggregated in many regions of the mutant fibers, indicating that cytoskeleton-mediated cellular transportation was impaired in the Li_1 fibers. Additionally, several proteins including a vacuolar-sorting protein SNF7, a γ-soluble nsf attachment protein, a coatomer-like protein involved in vesicle-mediated transport, and a glycolipid transfer protein (GLTP) capable of enhancing the intervesicular trafficking of glycosphingolipids *in vitro*[44] were also suppressed in Li_1 fibers. Suppression in the expression of these proteins may be another factor contributing to the disrupted intracellular trafficking in Li_1 fibers.

Calcium- and 14-3-3-Mediated Signaling Processes May Be Involved in the Regulation of Fiber Elongation. Elongation of the single-celled cotton fiber seemed to be a complex process involving various metabolic and regulatory pathways. Diverse signal transduction pathways were found to be involved in the regulation of fiber elongation including ethylene-, brassinosteroid (BR)- and auxin-mediated signalings.[5,8,45,46] We have previously reported that calcium signaling components such as calmodulin, CBL (calcineurin B-like protein) and CDPK (Ca^{2+}-dependent protein kinase) are up-regulated during fiber elongation.[47,48] Here we found that the expression of a calmodulin was highly suppressed in Li_1 fiber, thus further demonstrating the role of calcium signaling in fiber elongation.

The 14-3-3 proteins are implicated in the regulation of various cellular processes as well as in the integration of calcium signaling and other different signaling pathways.[49] Previously, Yang et al. observed the enhanced expression of a 14-3-3 protein in the elongating fibers.[6] In this work, we found that several 14-3-3 isoforms were down-regulated in the Li_1 fibers. Together, these results indicated that signaling process involving 14-3-3 proteins may have a critical role in regulating cotton fiber elongation.

Elongation Deficiency of Li_1 Fiber Is Related with ER Stress. Secretory and transmembrane proteins are synthesized in the endoplasmic reticulum (ER) in eukaryotic cells. When protein folding is affected, unfolded or misfolded proteins accumulate in the ER and cause ER stress that in turn activates the signal-transduction pathways referred as the unfolded protein response (UPR).[50] In mammals and yeast, protein disulfide isomerases (PDIs) and calreticulin are key ER chaperons activated during UPR.[51−54] However, little is known about their roles responding to ER stress in plants. In the Li_1 fibers, three isotypes of PDIs and one calreticulin were abundantly increased. PDIs are major folding catalysts in the eukaryotic ER, where they are responsible for the formation, breakage or shuffling of disulfide bonds in substrate polypeptides and are important chaperones in the secretory pathway.[55] Calreticulin plays important roles in variety processes such as Ca^{2+} signaling and protein folding specific for glycoproteins in ER.[56] Increased expression of the above-mentioned proteins indicated that ER-stress was caused in the Li_1 fiber due to the mutation. Coincidentally, Davidonis found that treatment of 2−6 DPA cotton fiber with tunicamycin, an agent causing ER stress, resulted in inhibited fiber elongation.[57]

Elongation Defect of Li_1 Fiber Is Associated with Stress Response. About one-third of the up-regulated proteins in the Li_1 mutant corresponded to the stress-responsive proteins. Most of these proteins are involved in the control of cellular redox homeostasis or detoxification in response to the environmental stresses, including the nucleoredoxin, ascorbate peroxidase, glutathione reductase, polyphenol oxidase and alcohol dehydrogenase. Apart from them, two germin-like proteins (GLPs) were significantly up-regulated. It has been shown that germins and GLPs are associated with the extracellular matrix and play various roles in plant development and defense.[58] An EF-Tu that is known to be a stress-responsive protein and two other stress-inducible proteins were also found to be induced in Li_1 fibers.

Growing evidence suggests that the ability of plant cells to sense defects in cell expansion resulting from an alteration in cell wall composition or integrity is closely linked to the activation of cellular signaling events, such as jasmonic acid- and ethylene-dependent stress and defense responses.[59−62] For example, a cell expansion mutant (*cob*) was found to invoke cellular defense responses in *Arabidopsis thaliana*. It was proposed that cell wall abnormality, caused by functional loss of the glycosylphosphatidylinositol (GPI)-anchored protein, could produce a damaged signal and an increase in the stress-responsive proteins.[63] In our study, we found that a number of stress-related proteins were activated in the fiber elongation mutant Li_1. Accompanying this, a more electron-dense cell wall in Li_1 fiber was observed. These findings provide another line of evidence to support the hypothesis that the cell expansion and stress response may be coordinately regulated through cell wall-mediated signals in plants.

Conclusions

By comparative proteomic study of the short-lint fiber mutant (Li_1) with its wild-type and by virtue of the established local EST data-assisted MS/MS analysis, we have identified several functional categories of cotton fiber elongation-related proteins. Suppression of a large number of cytoskeleton-related proteins and the deformed cytoskeleton structures along with disrupted intracellular trafficking in the Li_1 fibers emphasize the critical functions of these proteins in fiber development. The remarkable down-regulation of HSP90 expression in Li_1 fibers and the inhibition of fiber elongation by HSP90-specific inhibitor revealed an important role of this family of molecular chaperons in fiber elongation. The decreased expression of the signaling molecules such as calmodulin and 14-3-3 proteins indicated the participation of the related pathways in the signaling network regulating fiber growth. Finally, the up-regulated expression of the proteins involved in UPR and stress responses provided useful clues for further studies on the relationships between these cellular responses and plant cell elongation. Taken together, this research presents an important line of evidence showing the factors with deficient elongation of Li_1 fibers, and provides a substantial contribution to a deeper elucidation of the mechanisms governing cotton fiber elongation.

Acknowledgment. This work is supported by grants from the Ministry of Agriculture of China for transgenic research (Grant No. 2008ZX08009-003), the "863" High Technology Development Program (Grant No: 2006AA10A109-3) and the National Key Basic Research Program of China (Grant No: 2004CB117304). We are grateful to Prof. Jin-Yuan Liu (Tsinghua University) for helpful discussion of this study and to the Institute of Cotton, Chinese Academy of Agricultural Sciences for the Li_1 seeds. We also thank Dr. Chun-Li Li, Ms Jing-Nan Liang, and Dr Yin-Hong Zhang for their technical assistance with SEM, TEM, and confocal microscopy analyses.

Note Added after ASAP Publication. This paper was published on the Web on Dec 3, 2009, with errors on Table 1 and Figure 3. The corrected version was reposted on Jan 6, 2010.

References

(1) Basra, A. S.; Malik, C. P. Development of the cotton fiber. *Int. Rev. Cytol.* **1984**, *89*, 65–113.

(2) Ryser, U., Cotton fiber initiation and histodifferentiation. In *Cotton Fibers: Developmental Biology, Quality Improvement, and Textile Processing*; Basra, A. S., Ed.; Food Products Press: New York, 1999; pp 1−45.

(3) Kim, H. J.; Triplett, B. A. Cotton fiber growth in planta and in vitro. Models for plant cell elongation and cell wall biogenesis. *Plant Physiol.* **2001**, *127* (4), 1361–1366.

(4) Arpat, A. B.; Waugh, M.; Sullivan, J. P.; Gonzales, M.; Frisch, D.; Main, D.; Wood, T.; Leslie, A.; Wing, R. A.; Wilkins, T. A. Functional genomics of cell elongation in developing cotton fibers. *Plant Mol. Biol.* **2004**, *54* (6), 911–929.

(5) Shi, Y. H.; Zhu, S. W.; Mao, X. Z.; Feng, J. X.; Qin, Y. M.; Zhang, L.; Cheng, J.; Wei, L. P.; Wang, Z. Y.; Zhu, Y. X. Transcriptome profiling, molecular biological, and physiological studies reveal a major role for ethylene in cotton fiber cell elongation. *Plant Cell* **2006**, *18* (3), 651–664.

(6) Yang, Y. W.; Bian, S. M.; Yao, Y.; Liu, J. Y. Comparative Proteomic Analysis Provides New Insights into the Fiber Elongating Process in Cotton. *J. Proteome Res.* **2008**, *7* (11), 4623–4637.

(7) Li, H. B.; Qin, Y. M.; Pang, Y.; Song, W. Q.; Mei, W. Q.; Zhu, Y. X. A cotton ascorbate peroxidase is involved in hydrogen peroxide homeostasis during fibre cell development. *New Phytol.* **2007**, *175* (3), 462–471.

(8) Luo, M.; Xiao, Y.; Li, X.; Lu, X.; Deng, W.; Li, D.; Hou, L.; Hu, M.; Li, Y.; Pei, Y. GhDET2, a steroid 5alpha-reductase, plays an important role in cotton fiber cell initiation and elongation. *Plant J.* **2007**, *51* (3), 419–430.

(9) Li, X. B.; Fan, X. P.; Wang, X. L.; Cai, L.; Yang, W. C. The cotton ACTIN1 gene is functionally expressed in fibers and participates in fiber elongation. *Plant Cell* **2005**, *17* (3), 859–875.

(10) Ruan, Y. L.; Llewellyn, D. J.; Furbank, R. T. Suppression of sucrose synthase gene expression represses cotton fiber cell initiation, elongation, and seed development. *Plant Cell* **2003**, *15* (4), 952–964.

(11) Griffee, Fred.; Ligon, L. L. Occurrence of "lintless" cotton plants and the inheritance of the character "lintless. *J. Am. Soc. Agron.* **1929**, *21*, 711–717.

(12) Kohel, R. J.; Narbuth, E. V.; Benedict, C. R. Fiber development of ligon lintless-2 mutant of cotton. *Crop Sci.* **1992**, *32* (3), 733–735.

(13) Kohel, R. J.; Quisenbe, Je.; Benedict, C. R. Fiber elongation and dry weight changes in mutant lines of cotton. *Crop Sci.* **1974**, *14* (3), 471–474.

(14) Kohel, R. J. Linkage tests in upland cotton *Gossypium hirsutum L0.2. Crop Sci.* **1972**, *12* (1), 66–69.

(15) Karaca, M.; Saha, S.; Jenkins, J. N.; Zipf, A.; Kohel, R.; Stelly, D. M. Simple sequence repeat (SSR) markers linked to the Ligon lintless (Li-1) mutant in cotton. *J. Hered.* **2002**, *93* (3), 221–224.

(16) Du, X.-M. Early development of the fiber and inheritance of fiber mutants in upland cotton (*Gossypium hirsutum* L.). PhD thesis Nanjing Agricultural University, Nanjing, China, 1998.

(17) Triplett, B. A.; Busch, W. H.; Goynes, W. R. Ovule and suspension-culture of a cotton fiber development mutant. *In Vitro Cellular & Developmental Biology* **1989**, *25* (2), 197–200.

(18) Beasley, C. A.; Ting, I. P. Effects of plant-growth substances on in-vitro fiber development from fertilized cotton ovules. *Am. J. Bot.* **1973**, *60* (2), 130–139.

(19) Gao, P.; Zhao, P.-M.; Wang, J.; Wang, H.-Y.; Wu, X.-M.; Xia, G.-X. Identification of genes preferentially expressed in cotton fibers: A possible role of calcium signaling in cotton fiber elongation. *Plant Sci. (Oxford)* **2007**, *173* (1), 61–69.

(20) Yao, Y.; Yang, Y. W.; Liu, J. Y. An efficient protein preparation for proteomic analysis of developing cotton fibers by 2-DE. *Electrophoresis* **2006**, *27* (22), 4559–4569.

(21) Chen, Z. Z.; Xue, C. H.; Zhu, S.; Zhou, F. F.; Ling, X. F. B.; Liu, G. P.; Chen, L. B. GoPipe: Streamlined Gene Ontology annotation for batch anonymous sequences with statistics. *Prog. Biochem. Biophys.* **2005**, *32* (2), 187–190.

(22) Bradford, M. M. Rapid and sensitive method for quantitation of microgram quantities of protein utilizing principle of protein-dye binding. *Anal. Biochem.* **1976**, *72* (1−2), 248–254.

(23) Seagull, R. W. The effects of microtubule and microfilament disrupting agents on cytoskeletal arrays and wall deposition in developing cotton fibers. *Protoplasma* **1990**, *159* (1), 44–59.

(24) Preuss, M. L.; Delmer, D. P.; Liu, B. The cotton kinesin-like calmodulin-binding protein associates with cortical microtubules in cotton fibers. *Plant Physiol.* **2003**, *132* (1), 154–160.

(25) Pradet-Balade, B.; Boulme, F.; Beug, H.; Mullner, E. W.; Garcia-Sanz, J. A. Translation control: bridging the gap between genomics and proteomics. *Trends Biochem. Sci.* **2001**, *26* (4), 225–229.

(26) Greenbaum, D.; Colangelo, C.; Williams, K.; Gerstein, M. Comparing protein abundance and mRNA expression levels on a genomic scale. *Genome Biol.* **2003**, *4* (9), 8.

(27) Yan, S. P.; Zhang, Q. Y.; Tang, Z. C.; Su, W. A.; Sun, W. N. Comparative proteomic analysis provides new insights into chilling stress responses in rice. *Mol. Cell. Proteomics* **2006**, *5* (3), 484–496.

(28) Greenbaum, D.; Colangelo, C.; Williams, K.; Gerstein, M. Comparing protein abundance and mRNA expression levels on a genomic scale. *Genome Biol.* **2003**, *4* (9), 117.

(29) Chen, G.; Gharib, T. G.; Huang, C. C.; Taylor, J. M.; Misek, D. E.; Kardia, S. L.; Giordano, T. J.; Iannettoni, M. D.; Orringer, M. B.; Hanash, S. M.; Beer, D. G. Discordant protein and mRNA expression in lung adenocarcinomas. *Mol. Cell. Proteomics* **2002**, *1* (4), 304–313.

(30) Gygi, S. P.; Rochon, Y.; Franza, B. R.; Aebersold, R. Correlation between protein and mRNA abundance in yeast. *Mol. Cell. Biol.* **1999**, *19* (3), 1720–1730.

(31) Anderson, L.; Seilhamer, J. A comparison of selected mRNA and protein abundances in human liver. *Electrophoresis* **1997**, *18* (3−4), 533–537.

(32) Bolte, S.; Talbot, C.; Boutte, Y.; Catrice, O.; Read, N. D.; Satiat-Jeunemaitre, B. FM-dyes as experimental probes for dissecting vesicle trafficking in living plant cells. *J. Microsci.-Oxf.* **2004**, *214*, 159–173.

(33) Schulte, T. W.; Akinaga, S.; Soga, S.; Sullivan, W.; Stensgard, B.; Toft, D.; Neckers, L. M. Antibiotic radicicol binds to the N-terminal domain of Hsp90 and shares important biologic activities with geldanamycin. *Cell Stress Chaperones* **1998**, *3* (2), 100–108.

(34) Sangster, T. A.; Queitsch, C. The HSP90 chaperone complex, an emerging force in plant development and phenotypic plasticity. *Curr. Opin. Plant Biol.* **2005**, *8* (1), 86–92.

(35) Sorokin, A. V.; Kim, E. R.; Ovchinnikov, L. P. Nucleocytoplasmic transport of proteins. *Biochemistry (Mosc)* **2007**, *72* (13), 1439–57.

(36) Vernoud, V.; Horton, A. C.; Yang, Z.; Nielsen, E. Analysis of the small GTPase gene superfamily of Arabidopsis. *Plant Physiol.* **2003**, *131* (3), 1191–1208.

(37) Kim, S. H.; Arnold, D.; Lloyd, A.; Roux, S. J. Antisense expression of an Arabidopsis ran binding protein renders transgenic roots hypersensitive to auxin and alters auxin-induced root growth and development by arresting mitotic progress. *Plant Cell* **2001**, *13* (12), 2619–2630.

(38) Kim, S. H.; Roux, S. J. An Arabidopsis Ran-binding protein, AtRanBP1c, is a co-activator of Ran GTPase-activating protein and requires the C-terminus for its cytoplasmic localization. *Planta* **2003**, *216* (6), 1047–1051.

(39) Mortimer, J. C.; Laohavisit, A.; Macpherson, N.; Webb, A.; Brownlee, C.; Battey, N. H.; Davies, J. M. Annexins: multifunctional components of growth and adaptation. *J. Exp. Bot.* **2008**, *59* (3), 533–544.

(40) Konopka-Postupolska, D. Annexins: putative linkers in dynamic membrane-cytoskeleton interactions in plant cells. *Protoplasma* **2007**, *230* (3−4), 203–215.

(41) Ramachandran, S.; Christensen, H. E.; Ishimaru, Y.; Dong, C. H.; Chao-Ming, W.; Cleary, A. L.; Chua, N. H. Profilin plays a role in cell elongation, cell shape maintenance, and flowering in Arabidopsis. *Plant Physiol.* **2000**, *124* (4), 1637–1647.

(42) Li, X. B.; Cai, L.; Cheng, N. H.; Liu, J. W. Molecular characterization of the cotton GhTUB1 gene that is preferentially expressed in fiber. *Plant Physiol.* **2002**, *130* (2), 666–674.

(43) He, X. C.; Qin, Y. M.; Xu, Y.; Hu, C. Y.; Zhu, Y. X. Molecular cloning, expression profiling, and yeast complementation of 19 beta-tubulin cDNAs from developing cotton ovules. *J Exp Bot* **2008**, *59* (10), 2687–2695.

(44) West, G.; Viitanen, L.; Alm, C.; Mattjus, P.; Salminen, T. A.; Edqvist, J. Identification of a glycosphingolipid transfer protein GLTP1 in Arabidopsis thaliana. *FEBS J.* **2008**, *275* (13), 3421–3437.

(45) Gou, J. Y.; Wang, L. J.; Chen, S. P.; Hu, W. L.; Chen, X. Y. Gene expression and metabolite profiles of cotton fiber during cell elongation and secondary cell wall synthesis. *Cell Res.* **2007**, *17* (5), 422–434.

(46) Sun, Y.; Veerabomma, S.; Abdel-Mageed, H. A.; Fokar, M.; Asami, T.; Yoshida, S.; Allen, R. D. Brassinosteroid regulates fiber development on cultured cotton ovules. *Plant Cell Physiol.* **2005**, *46* (8), 1384–1391.
(47) Gao, P.; Zhao, P. M.; Wang, J.; Wang, H. Y.; Du, X. M.; Wang, G. L.; Xia, G. X. Co-expression and preferential interaction between two calcineurin B-like proteins and a CBL-interacting protein kinase from cotton. *Plant Physiol. Biochem.* **2008**, *46* (10), 935–940.
(48) Huang, Q. S.; Wang, H. Y.; Gao, P.; Wang, G. Y.; Xia, G. X. Cloning and characterization of a calcium dependent protein kinase gene associated with cotton fiber development. *Plant Cell Rep.* **2008**, *27* (12), 1869–1875.
(49) Chow, C. W.; Davis, R. J. Integration of calcium and cyclic AMP signaling pathways by 14-3-3. *Mol. Cell. Biol.* **2000**, *20* (2), 702–712.
(50) Urade, R. Cellular response to unfolded proteins in the endoplasmic reticulum of plants. *FEBS J.* **2007**, *274* (5), 1152–1171.
(51) Ni, M.; Lee, A. S. ER chaperones in mammalian development and human diseases. *FEBS Lett.* **2007**, *581* (19), 3641–3651.
(52) Xu, P.; Raden, D.; Doyle, F. J.; Robinson, A. S. Analysis of unfolded protein response during single-chain antibody expression in Saccaromyces cerevisiae reveals different roles for BiP and PDI in folding. *Metab. Eng.* **2005**, *7* (4), 269–279.
(53) Dorner, A. J.; Wasley, L. C.; Raney, P.; Haugejorden, S.; Green, M.; Kaufman, R. J. The stress response in chinese-hamster ovary cells - regulation of ERP72 and protein disulfide isomerase expression and secretion. *J. Biol. Chem.* **1990**, *265* (35), 22029–22034.
(54) Uehara, T.; Nakamura, T.; Yao, D. D.; Shi, Z. Q.; Gu, Z. Z.; Ma, Y. L.; Masliah, E.; Nomura, Y.; Lipton, S. A. S-Nitrosylated protein-disulphide isomerase links protein misfolding to neurodegeneration. *Nature* **2006**, *441* (7092), 513–517.
(55) Lees, W. J. Small-molecule catalysts of oxidative protein folding. *Curr. Opin. Chem. Biol.* **2008**, *12* (6), 740–745.
(56) Williams, D. B. Beyond lectins: the calnexin/calreticulin chaperone system of the endoplasmic reticulum. *J. Cell Sci.* **2006**, *119* (4), 615–623.
(57) Davidonis, G. Cotton fiber growth and development invitro - effects of tunicamycin and monensin. *Plant Sci.* **1993**, *88* (2), 229–236.
(58) Berna, A.; Bernier, F. Regulation by biotic and abiotic stress of a wheat germin gene encoding oxalate oxidase, a H2O2-producing enzyme. *Plant Mol. Biol.* **1999**, *39* (3), 539–549.
(59) Tao, Y.; Xie, Z. Y.; Chen, W. Q.; Glazebrook, J.; Chang, H. S.; Han, B.; Zhu, T.; Zou, G. Z.; Katagiri, F. Quantitative nature of Arabidopsis responses during compatible and incompatible interactions with the bacterial pathogen Pseudomonas syringae. *Plant Cell* **2003**, *15* (2), 317–330.
(60) Zhong, R. Q.; Kays, S. J.; Schroeder, B. P.; Ye, Z. H. Mutation of a Chitinase-like gene causes ectopic deposition of lignin, aberrant cell shapes, and overproduction of ethylene. *Plant Cell* **2002**, *14* (1), 165–179.
(61) Ellis, C.; Turner, J. G. The Arabidopsis mutant cev1 has constitutively active jasmonate and ethylene signal pathways and enhanced resistance to pathogens. *Plant Cell* **2001**, *13* (5), 1025–1033.
(62) Ellis, C.; Karafyllidis, I.; Wasternack, C.; Turner, J. G. The Arabidopsis mutant cev1 links cell wall signaling to jasmonate and ethylene responses. *Plant Cell* **2002**, *14* (7), 1557–1566.
(63) Ko, J. H.; Kim, J. H.; Jayanty, S. S.; Howe, G. A.; Han, K. H. Loss of function of COBRA, a determinant of oriented cell expansion, invokes cellular defence responses in Arabidopsis thaliana. *J. Exp. Bot.* **2006**, *57* (12), 2923–2936.

PR900975T